

Spin Hall Effect of Light via Momentum-Space Topological Vortices around Bound States in the Continuum

Jiajun Wang,¹ Lei Shi,^{1,2,3,*} and Jian Zi^{1,2,3,†}

¹State Key Laboratory of Surface Physics, Key Laboratory of Micro- and Nano-Photonic Structures (Ministry of Education) and Department of Physics, Fudan University, Shanghai 200433, China

²Institute for Nanoelectronic Devices and Quantum Computing, Fudan University, Shanghai 200438, China

³Collaborative Innovation Center of Advanced Microstructures, Nanjing University, Nanjing 210093, China

 (Received 11 July 2022; accepted 2 November 2022; published 30 November 2022)

Optical bound states in the continuum (BICs) are exotic topological defects in photonic crystal slabs, carrying polarization topological vortices in momentum space. The topological vortex configurations not only topologically protect the infinite radiation lifetime of BICs, but also intrinsically contain many unexploited degrees of freedom for light manipulation originating from BICs. Here, we theoretically propose and experimentally demonstrate the spin Hall effect of light in photonic crystal slabs via momentum-space topological vortices around BICs. The strong spin-orbit interactions of light are induced by using the topological vortices around BICs, introducing both wave-vector-dependent Pancharatnam-Berry phase gradients and cross-polarized resonant phase gradients to the spinning light beam, which lead to spin-dependent in-plane-oblique lateral light beam shifts. Our work reveals intriguing spin-related topological effects around BICs, opening an avenue toward applications of BICs in integrated spin-optical devices and information processing.

DOI: 10.1103/PhysRevLett.129.236101

Optical bound states in the continuum (BICs) in photonic crystal (PhC) slabs [1,2], being recently found as topological defects [3] in momentum space, have aroused great interest and been widely explored. Around BICs, the states of polarization (SOPs) of radiative modes form vortices in momentum space [4–8]. Being the vortex singularity, each BIC carries a topological charge, which is characterized by the winding number of SOPs around the BIC [5]. Many BIC-related topological properties in momentum space have been reported in various research, e.g., the momentum-space dynamic evolution of topological charges [9–14] and the multipolar origin of BICs [15,16], with various applications in ultrahigh-Q cavities [17–22], unidirectional radiation [23], zero-index materials [24,25], vortex lasers [26], etc. Furthermore, recent research shows that the topological vortices around BICs have the ability to generate optical vortex beams [27,28]. This intriguing finding achieves the transformation from momentum-space polarization vortex of PhC slabs to phase vortex of light beams, showing that topological vortices can provide a new form of spin-orbit interactions (SOIs) of light in PhC slabs.

SOIs of light are inherent in all basic optical processes, underlying many unique physical properties of light [29–35]. In PhC slabs, the SOI effects emerge during the resonance process between light in free space and radiative modes. At this point, the topological vortices around BICs can offer new degrees of freedom to manipulate the SOIs of light. The polarization anisotropy in momentum space can introduce strong SOIs via mode

conversion. For instance, the lower panel of Fig. 1 shows the topological vortex in momentum space with a central BIC of -1 topological charge. Ensured by the nontrivial topological configuration of the BIC, the orientations of SOPs of radiative modes rapidly vary around the BIC. When the spinning light in free space propagates onto PhC slabs and couples with these radiative modes, the caused responses of the induced SOI in PhC slabs can be divided into two parts: on the one hand, the polarization anisotropy

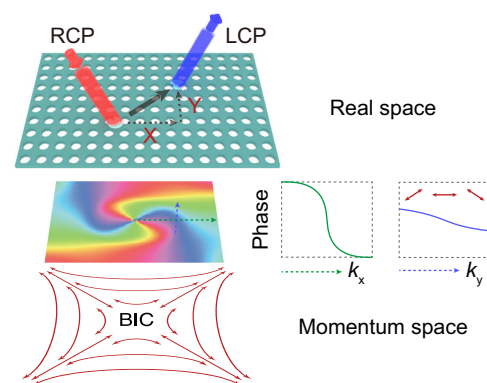


FIG. 1. Lower panel: topological vortex around the BIC in momentum space. Middle panel: cross-polarized phase distribution in momentum space under circularly polarized incidence. Green line shows the cross-polarized resonant phase along the k_x direction; cyan line shows the PB phase along the k_y direction. Upper panel: schematic view of the spin Hall effect of light.

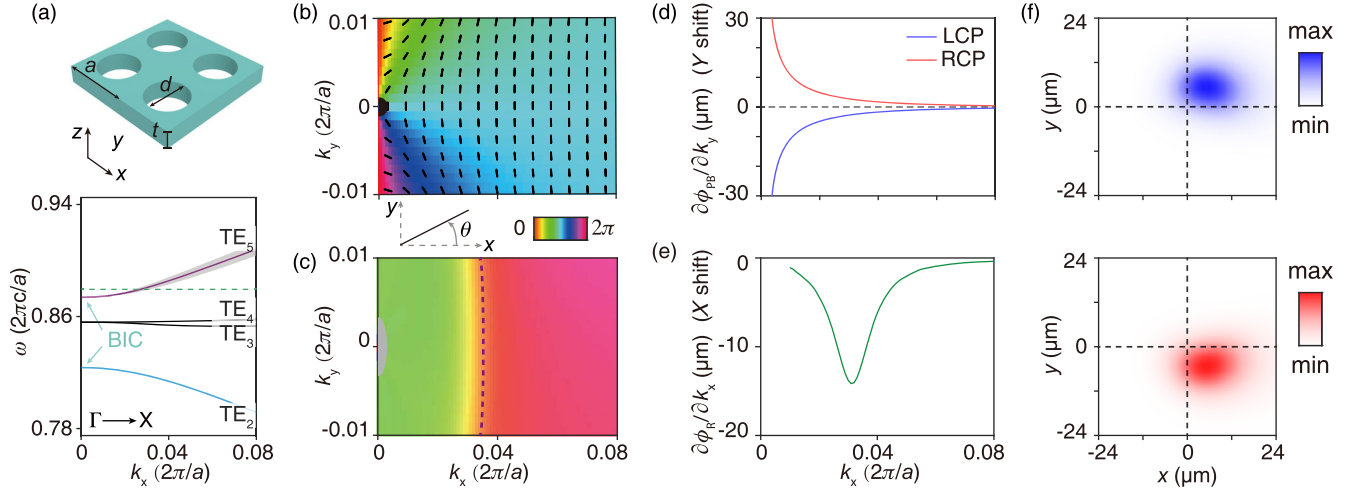


FIG. 2. (a) Upper panel: diagram of the PhC slab. Lower panel: calculated band structure along the Γ - X direction. (b) Momentum-space polarization map of the TE_5 band and the induced PB phase (from the RCP to LCP). (c) Momentum-space cross-polarized resonant phase distribution at a single wavelength. (d) PB phase gradients in the k_y direction at different k_x ($k_y = 0$), which leads to the Y shift. The PB phase gradient from the RCP to LCP (marked as blue color) is opposite to that from the LCP to RCP (marked as red color). (e) Cross-polarized resonant phase gradients in the k_x direction at different k_x ($k_y = 0$) from Fig. 2(c), which leads to the X shift. (f) Top view of the realized spin Hall effect of light by simulation.

induces Pancharatnam-Berry (PB) phase [27,36,37] to the cross-polarized converted light via the mode conversion. The induced PB phases are directly associated with the orientations of SOPs and the spin of the incident light. On the other hand, the cross-polarized conversion via the resonance between the incident light and the radiative mode would also induce a wave-vector-dependent cross-polarized resonant phase, offering a larger degree of freedom for affecting the spinning light. As a manifestation at a single wavelength, the middle panel of Fig. 1 shows the SOI-introduced phase distribution in momentum space for the cross-polarized converted light. Accompanied by the shown wave-vector-dependent momentum-space phase distribution, the spin Hall effect of light is expected.

The general spin Hall effects of light include spin-dependent lateral beam shifts [38–41], angular deflection [41,42], and near-field propagation [43,44]. Among them, spin-dependent beam shifts have attracted much attention for both the fundamental science and potential applications in manipulating the spinning light [45,46]. Because of weak SOI at normal optical interfaces, spin Hall shifts are usually small, making them hard to observe. Recently, a few approaches have been proposed to enhance the spin Hall shifts, such as using metasurfaces [41,47,48], uniaxial crystals [49–51], or BIC in epsilon near-zero materials [52], while for conventional spin Hall shifts, shift directions are almost limited to be transverse to the incident plane.

Here, we theoretically propose and experimentally demonstrate that momentum-space topological vortices around BICs result in a novel spin Hall effect of light (spin-related in-plane-oblique lateral beam shifts) in which lateral shift directions can be distributed in all four quadrants.

For example, as exhibited in the upper panel of Fig. 1, when a right-handed circularly polarized (RCP) paraxial light beam shines onto the PhC slab along the X direction, the cross-polarized converted reflection light beam (left-handed circularly polarized, LCP) would be dragged by the PhC slab with a lateral shift. This lateral shift originates from SOI-induced phase gradients in momentum space, in which PB phase gradients lead to the Y -direction transverse shift and cross-polarized resonant phase gradients lead to the X -direction longitudinal shift.

To start, using coupled mode theory, we can describe the reflection via topological vortices around BICs from momentum-space perspective. Considering that the electromagnetic wave of a certain in-plane \mathbf{k}_{\parallel} shines onto a PhC slab, we can formulate the reflection as

$$\begin{aligned}
 |E_{\text{out}}\rangle &= S|E_{\text{in}}\rangle \\
 &= \begin{bmatrix} r_{ll}(\mathbf{k}_{\parallel}) & r_{lr}(\mathbf{k}_{\parallel})e^{2i\theta(\mathbf{k}_{\parallel})} \\ r_{rl}(\mathbf{k}_{\parallel})e^{-2i\theta(\mathbf{k}_{\parallel})} & r_{rr}(\mathbf{k}_{\parallel}) \end{bmatrix} |E_{\text{in}}\rangle \quad (1)
 \end{aligned}$$

on a helical basis, where the subscripts $l(r)$ refer to the LCP and RCP. Here, S is the general scattering matrix of the reflection; $|E_{\text{in}}\rangle$, $|E_{\text{out}}\rangle$ are Jones vectors of the incident and reflected light; r_{ll} , r_{lr} , r_{rl} , r_{rr} are reflection coefficients; and $\theta(\mathbf{k}_{\parallel})$ is defined as the azimuthal angle of the SOP of corresponding resonant radiative mode, as shown in the bottom inset of Fig. 2(b). From matrix S , we can see that the off-diagonal elements are with additional phase factors $e^{\pm 2i\theta(\mathbf{k}_{\parallel})}$, originating from the geometric phase, i.e., a PB phase. The nontrivial phases are carried by cross-polarized converted parts of the reflected light and have opposite

signs for two different cross-polarized converted parts. As a manifestation, when an RCP light shines on the PhC slab, the reflection phase of the cross-polarized converted light can be further written as

$$\varphi_{lr}(\mathbf{k}_{\parallel}) = \text{angle}[r_{lr}(\mathbf{k}_{\parallel})] + 2\theta(\mathbf{k}_{\parallel}). \quad (2)$$

Besides the PB phase, there is an additional cross-polarized resonant phase, being an accompanying result of SOIs in PhC slabs due to the nonlocal resonance. These two wave-vector-variant phases lead to large momentum-space phase gradients and hence result in real-space lateral shifts with the relative shift $\mathbf{R} = -[\partial\varphi(\mathbf{k}_{\parallel})/\partial\mathbf{k}]$, based on the fact that the momentum space and the real space are a pair of reciprocal spaces [53–56]. Various spin-related phase gradients exist in topological vortices around BICs, offering large degrees of freedom to realize spin Hall shifts.

Considering a simple case in Fig. 1, with the incident RCP light with a in-plane \mathbf{k}_{\parallel} along Γ - X direction, the beam shift for the cross-polarized converted light \mathbf{R}_L can be described as

$$\mathbf{R}_L = \frac{2\alpha_{v_g}\gamma}{4\gamma^2 + (|\mathbf{k}_{\parallel}| - k_0)^2} \hat{\mathbf{x}} - \frac{2\partial\theta(\mathbf{k}_{\parallel})}{\partial k_y} \hat{\mathbf{y}} = \mathbf{X} + \mathbf{Y}, \quad (3)$$

where $\hat{\mathbf{x}}$ and $\hat{\mathbf{y}}$ are unit vectors along the X and Y directions, respectively. Here, k_0 is the wave vector of the resonant radiative mode along the k_x direction, γ refers to the radiation loss, and α_{v_g} is the group velocity factor of the radiative mode [$\alpha_{v_g} = 1(-1)$ for the positive (negative) group velocity]. The second term corresponds to the PB phase gradient, leading to a Y -direction transverse shift similar to conventional spin Hall shifts. The first term corresponds to the cross-polarized resonant phase gradient, leading to the X -direction longitudinal shift. This additional cross-polarized resonant phase term enables the spin Hall shift direction to have a new combination of X direction. A detailed explanation of the coupled mode theory is provided in Supplemental Material [57].

To give a specific example for our proposed theory, we consider a PhC slab with C_{4v} symmetry. The PhC structure consists of a freestanding silicon nitride (refractive index = 2) slab with a square lattice of cylindrical holes. As shown in Fig. 2(a), the thickness t is 100 nm, the period a is 700 nm, and the diameter d is 470 nm. Figure 2(a) also shows calculated transverse electric (TE)-like band structures along the Γ - X direction. For the second TE-like (TE₂) band and the fifth TE-like (TE₅) band, the symmetry-protected BIC is centred at Γ point. Here, we focus on the TE₅ band, in which the topological charge of the central BIC is -1 . Figure 2(b) exhibits a part of the topological vortex around the BIC in the TE₅ band, with SOPs marked by dark short lines. Around the BIC, the orientations θ of SOPs decrease along the counterclockwise loop, with the total winding angle being -2π .

The color map in Fig. 2(b) shows the induced PB phase distribution for cross-polarized conversion from the RCP to LCP. Along the Γ - X direction, there are negative PB phase gradients in the k_y direction [blue line in Fig. 2(d)], leading to positive Y -direction shifts. For the other case from the LCP to RCP, PB phase gradients change to be positive [red line in Fig. 2(d)], leading to negative Y -direction shifts. The absolute values of PB phase gradients decrease along with the increasing wave vector, making the Y -direction beam shifts to also be wave-vector-dependent.

The nonlocally resonant behaviors of the radiative modes around BICs allow us to further induce cross-polarized resonant phases. Figure 2(c) presents the cross-polarized resonant phase distribution from the RCP to LCP at 796 nm [the dashed line in Fig. 2(a)], where the dashed curve corresponds to the isofrequency contour of the TE₅ band. Because of the positive dispersion of the TE₅ band ($\alpha_{v_g} = 1$), the corresponding cross-polarized resonant phase gradients are negative from Eq. (3), referring to positive X -direction shifts. As expected, the cross-polarized resonant phase decreases rapidly in the vicinity of radiative modes [Fig. 2(c)] and along the Γ - X direction there are negative cross-polarized resonant phase gradients in the k_x direction [green line in Fig. 2(e)]. The absolute phase gradient approaches the maximum when the incidence is on resonance ($k_x = k_0$), in accordance with Eq. (3). Note that, for the other case from the LCP to RCP, the cross-polarized resonant phase gradients remain the same.

The spin Hall effect of light induced by the topological vortex around the BIC is then confirmed by simulations upon a finite-sized PhC slab consisting of 136×136 unit cells. A circularly polarized Gaussian beam is shined at the center ($x = 0, y = 0$) of the sample, with the wavelength of 796 nm and the incidence on resonance. The divergence angle of the beam is about 1.3° and the beam waist radius is $10 \mu\text{m}$. Figure 2(f) exhibits the top view of the cross-polarized converted reflected light. As shown in the upper panel, when the incidence is RCP, the reflected LCP light beam is shifted with a positive X and a positive Y . For the other case from the LCP to RCP, the cross-polarized converted light beam is shifted with a positive X and a negative Y . The results agree with the predication from the phase gradients. We also give similar discussions on the topological vortex around the BIC of $+1$ topological charge in the TE₂ band. Details are in Supplemental Material [57].

To confirm the spin Hall effect of light experimentally, we fabricated the designed PhC slab (sample size $200 \times 200 \mu\text{m}^2$). For optical measurements, we built a homemade Fourier-optics-based [62] measurement system, which could work in two modes: an angle-resolved spectrometer mode and a real-space imaging mode. Details are in Supplemental Material [57].

First, using the angle-resolved spectrometer mode, we measured the angle-resolved reflectance spectra of fabricated samples. Figure 3(a) shows measured angle-resolved

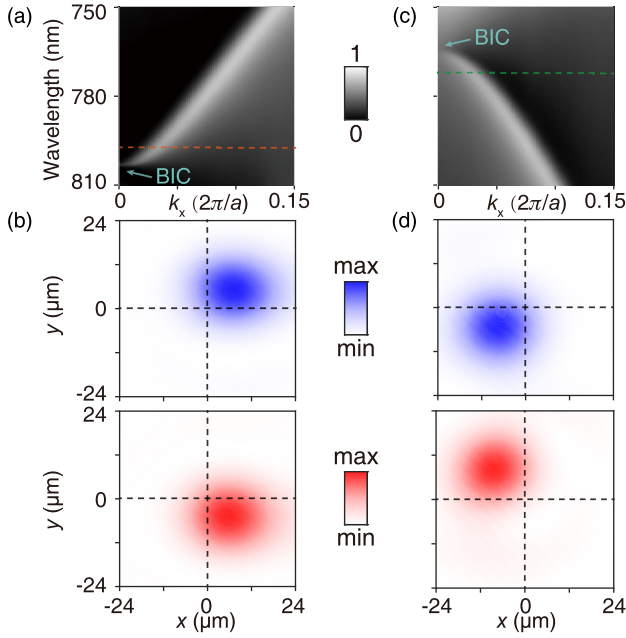


FIG. 3. (a) Angle-resolved *s*-polarized reflectance spectra of the TE₅ band along the Γ -*X* direction. (b) Image of the spin-dependent lateral shifts via the topological vortex in the TE₅ band. (c) Angle-resolved *s*-polarized reflectance spectra of the TE₂ band along the Γ -*X* direction. (d) Image of the spin-dependent lateral shifts via the topological vortex in the TE₂ band.

reflectance spectra of the TE₅ band of the fabricated sample with designed parameters in Fig. 2. The spectra are along the Γ -*X* direction and with *s*-polarized incidence, which agrees well with the simulated band structure of the TE₅ band in Fig. 2(a). We also measured angle-resolved reflectance spectra of the TE₂ band along the Γ -*X* direction, as shown in Fig. 3(c). Note that, to make the TE₂ band suit the tunable range of the laser, another sample was fabricated by changing the period *a* and diameter *d* to be 620 and 430 nm, respectively. The vanishing point marked by the cyan arrow corresponds to the central BIC, which cannot be excited by the far-field incidence.

Then, by switching the system to the real-space imaging mode, we performed direct measurements of the spin Hall effect via the near-BIC radiative modes of the topological vortices. Figure 3(b) shows the spin-dependent lateral beam shifts via the topological vortex in the TE₅ band, where the blue (red) color map refers to the cross-polarized converted light from the RCP (LCP) to LCP (RCP). The wavelength of the tunable laser is set to be 797 nm, marked by orange dashed line in Fig. 3(a), and the incident angle is set to be on resonance. As measured light beam profiles show, the LCP light beam is shifted with a positive *X* and a positive *Y*, while the RCP light beam is shifted with a positive *X* and a negative *Y*. The results are in good accordance with our simulated results in Fig. 2(f). For comparison, Fig. 3(d) shows spin-dependent lateral beam shifts via the topological vortex in the TE₂ band, in which the laser wavelength

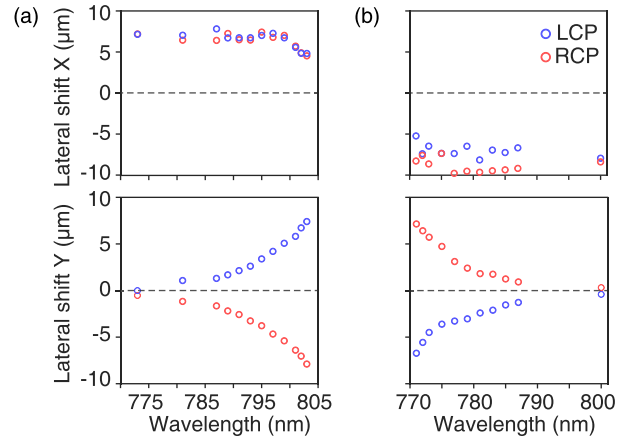


FIG. 4. Spin Hall effect of light at different wavelengths. (a) Lateral shifts via the topological vortex in the TE₅ band. (b) Lateral shifts via the topological vortex in the TE₂ band.

was set as 772 nm [green dashed line in Fig. 3(c)]. It could be seen that longitudinal lateral shifts are changed to the negative *X* direction, which are determined by the negative group velocity of the TE₂ band. And the LCP (RCP) light beam has a negative (positive) *Y* shift, being opposite to results in Fig. 3(b). The opposite spin-dependent responses of transverse lateral shifts can be understood by different topological configurations of BICs for the TE₂ band and the TE₅ band.

Finally, we measured the spin Hall effect at different wavelengths (Fig. 4), showing the wavelength dependence of the spin-dependent lateral shifts via topological vortices around BICs of +1 and −1 topological charge. The incident angle is set on resonance in each measurement. For longitudinal lateral shifts via a specific topological vortex around the BIC, the shift directions remain positive [upper panel of Fig. 4(a)] or negative [upper panel of Fig. 4(b)], which is in accordance with corresponding group velocity factors. For transverse lateral shifts along the *Y* direction, the absolute shifts depend on PB phase gradients of the on-resonance wave vectors. Hence, for the TE₅ band with a positive dispersion [Fig. 3(a)], as the wavelength increases, the on-resonance wave vector decreases to get closer to the central BIC to have larger PB phase gradients, leading to a larger absolute transverse lateral shift [lower panel of Fig. 4(a)]. And for the TE₂ band with a negative dispersion [Fig. 3(c)], the absolute transverse lateral shift gets smaller as the wavelength increases [lower panel of Fig. 4(b)]. In both cases, when the excited radiative mode is far away from the topological vortex center (the BIC), there are nearly negligible spin-dependent transverse lateral beam shifts. The simulations at different wavelengths are also provided in Supplemental Material [57].

Besides the fundamental interest, the research on spin Hall effect of light has led to many potential applications [46]. For this work, potential applications can include the light beam manipulation and precision sensing: on the one

hand, with the ultrathin structure thickness and the ability to realize large spin-dependent shifts, the proposed spin Hall effect can be used to develop PhC-slab-based microbeam shifters for the spinning light. On the other hand, BICs are sensitive to the environment; hence, the BIC-based spin Hall effect may also be applied to environment sensing like refractive index sensing. Certainly, more possible applications are expected in later research with deeper exploration.

In conclusion, we have exploited topological vortices around BICs to induce the spin Hall effect of light. Because of the strong SOI, large spin Hall shifts are realized via a 100-nm-thick PhC slab (a comparison with previous works is exhibited in Supplemental Material [57]). The cross-polarized resonant phase term offers a new degree of freedom to realize an additional X -direction shift. Combined with the vortex topological configurations around BICs, the spin-dependent in-plane-oblique lateral shifts were experimentally observed, with the shift directions distributed in all four quadrants. This work opens an unexplored avenue to realizing spin Hall effect of light via topological vortices around BICs, giving a promising way for on-chip applications on optical manipulation and spinoptics.

The work was supported by the China National Key Basic Research Program 2022YFA1404800 and National Science Foundation of China (No. 12234007 and No. 12221004). L. S. was further supported by Science and Technology Commission of Shanghai Municipality (No. 19XD1434600, No. 2019SHZDZX01, No. 19DZ2253000, No. 20501110500, and No. 21DZ1101500). We thank Dr. Wenzhe Liu for helpful discussions.

*Corresponding author.

lshi@fudan.edu.cn

†Corresponding author.

jzi@fudan.edu.cn

- [1] C. W. Hsu, B. Zhen, J. Lee, S.-L. Chua, S. G. Johnson, J. D. Joannopoulos, and M. Soljačić, *Nature (London)* **499**, 188 (2013).
- [2] C. W. Hsu, B. Zhen, A. D. Stone, J. D. Joannopoulos, and M. Soljačić, *Nat. Rev. Mater.* **1**, 16048 (2016).
- [3] N. D. Mermin, *Rev. Mod. Phys.* **51**, 591 (1979).
- [4] S. Fan and J. D. Joannopoulos, *Phys. Rev. B* **65**, 235112 (2002).
- [5] B. Zhen, C. W. Hsu, L. Lu, A. D. Stone, and M. Soljačić, *Phys. Rev. Lett.* **113**, 257401 (2014).
- [6] Y. Guo, M. Xiao, and S. Fan, *Phys. Rev. Lett.* **119**, 167401 (2017).
- [7] Y. Zhang, A. Chen, W. Liu, C. W. Hsu, B. Wang, F. Guan, X. Liu, L. Shi, L. Lu, and J. Zi, *Phys. Rev. Lett.* **120**, 186103 (2018).
- [8] H. M. Döeleman, F. Monticone, W. den Hollander, A. Alù, and A. F. Koenderink, *Nat. Photonics* **12**, 397 (2018).
- [9] W. Liu, B. Wang, Y. Zhang, J. Wang, M. Zhao, F. Guan, X. Liu, L. Shi, and J. Zi, *Phys. Rev. Lett.* **123**, 116104 (2019).
- [10] T. Yoda and M. Notomi, *Phys. Rev. Lett.* **125**, 053902 (2020).
- [11] W. Ye, Y. Gao, and J. Liu, *Phys. Rev. Lett.* **124**, 153904 (2020).
- [12] M. Kang, S. Zhang, M. Xiao, and H. Xu, *Phys. Rev. Lett.* **126**, 117402 (2021).
- [13] Y. Zeng, G. Hu, K. Liu, Z. Tang, and C.-W. Qiu, *Phys. Rev. Lett.* **127**, 176101 (2021).
- [14] W. Chen, Q. Yang, Y. Chen, and W. Liu, *Proc. Natl. Acad. Sci. U.S.A.* **118**, e2019578118 (2021).
- [15] W. Chen, Y. Chen, and W. Liu, *Phys. Rev. Lett.* **122**, 153907 (2019).
- [16] Z. Sadrieva, K. Frizyuk, M. Petrov, Y. Kivshar, and A. Bogdanov, *Phys. Rev. B* **100**, 115303 (2019).
- [17] K. Hirose, Y. Liang, Y. Kurosaka, A. Watanabe, T. Sugiyama, and S. Noda, *Nat. Photonics* **8**, 406 (2014).
- [18] A. Kodigala, T. Lepetit, Q. Gu, B. Bahari, Y. Fainman, and B. Kanté, *Nature (London)* **541**, 196 (2017).
- [19] K. Koshelev, S. Lepeshov, M. Liu, A. Bogdanov, and Y. Kivshar, *Phys. Rev. Lett.* **121**, 193903 (2018).
- [20] J. Jin, X. Yin, L. Ni, M. Soljačić, B. Zhen, and C. Peng, *Nature (London)* **574**, 501 (2019).
- [21] Z. Liu, Y. Xu, Y. Lin, J. Xiang, T. Feng, Q. Cao, J. Li, S. Lan, and J. Liu, *Phys. Rev. Lett.* **123**, 253901 (2019).
- [22] V. Ardizzone, F. Riminucci, S. Zanotti, A. Gianfrate, M. Efthymiou-Tsironi, D. Suárez-Forero, F. Todisco, M. De Giorgi, D. Trypogeorgos, G. Gigli *et al.*, *Nature (London)* **605**, 447 (2022).
- [23] X. Yin, J. Jin, M. Soljačić, C. Peng, and B. Zhen, *Nature (London)* **580**, 467 (2020).
- [24] M. Minkov, I. A. D. Williamson, M. Xiao, and S. Fan, *Phys. Rev. Lett.* **121**, 263901 (2018).
- [25] H. Tang, C. DeVault, S. A. Camayd-Muñoz, Y. Liu, D. Jia, F. Du, O. Mello, D. I. Vulis, Y. Li, and E. Mazur, *Nano Lett.* **21**, 914 (2021).
- [26] C. Huang, C. Zhang, S. Xiao, Y. Wang, Y. Fan, Y. Liu, N. Zhang, G. Qu, H. Ji, J. Han *et al.*, *Science* **367**, 1018 (2020).
- [27] B. Wang, W. Liu, M. Zhao, J. Wang, Y. Zhang, A. Chen, F. Guan, X. Liu, L. Shi, and J. Zi, *Nat. Photonics* **14**, 623 (2020).
- [28] M. Notomi, *Nat. Photonics* **14**, 595 (2020).
- [29] K. Y. Bliokh, D. Smirnova, and F. Nori, *Science* **348**, 1448 (2015).
- [30] Y. Tang, K. Li, X. Zhang, J. Deng, G. Li, and E. Brasselet, *Nat. Photonics* **14**, 658 (2020).
- [31] J. Eismann, L. Nicholls, D. Roth, M. A. Alonso, P. Banzer, F. Rodríguez-Fortuño, A. Zayats, F. Nori, and K. Bliokh, *Nat. Photonics* **15**, 156 (2021).
- [32] A. T. O’Neil, I. MacVicar, L. Allen, and M. J. Padgett, *Phys. Rev. Lett.* **88**, 053601 (2002).
- [33] G. Hu, X. Hong, K. Wang, J. Wu, H.-X. Xu, W. Zhao, W. Liu, S. Zhang, F. Garcia-Vidal, B. Wang *et al.*, *Nat. Photonics* **13**, 467 (2019).
- [34] N. Shitrit, I. Yulevich, E. Maguid, D. Ozeri, D. Veksler, V. Kleiner, and E. Hasman, *Science* **340**, 724 (2013).
- [35] J. Petersen, J. Volz, and A. Rauschenbeutel, *Science* **346**, 67 (2014).
- [36] M. V. Berry, *J. Mod. Opt.* **34**, 1401 (1987).
- [37] Z. Bomzon, G. Biener, V. Kleiner, and E. Hasman, *Opt. Lett.* **27**, 1141 (2002).
- [38] M. Onoda, S. Murakami, and N. Nagaosa, *Phys. Rev. Lett.* **93**, 083901 (2004).
- [39] O. Hosten and P. Kwiat, *Science* **319**, 787 (2008).

- [40] K. Y. Bliokh, A. Niv, V. Kleiner, and E. Hasman, *Nat. Photonics* **2**, 748 (2008).
- [41] X. Yin, Z. Ye, J. Rho, Y. Wang, and X. Zhang, *Science* **339**, 1405 (2013).
- [42] X. Ling, X. Zhou, X. Yi, W. Shu, Y. Liu, S. Chen, H. Luo, S. Wen, and D. Fan, *Light. Light.* **4**, e290 (2015).
- [43] J. Lin, J. B. Mueller, Q. Wang, G. Yuan, N. Antoniou, X.-C. Yuan, and F. Capasso, *Science* **340**, 331 (2013).
- [44] G. Zito, S. Romano, S. Cabrini, G. Calafiore, A. C. De Luca, E. Penzo, and V. Mocella, *Optica* **6**, 1305 (2019).
- [45] K. Y. Bliokh, F. J. Rodríguez-Fortuño, F. Nori, and A. V. Zayats, *Nat. Photonics* **9**, 796 (2015).
- [46] X. Ling, X. Zhou, K. Huang, Y. Liu, C.-W. Qiu, H. Luo, and S. Wen, *Rep. Prog. Phys.* **80**, 066401 (2017).
- [47] X. Ling, F. Guan, X. Cai, S. Ma, H.-X. Xu, Q. He, S. Xiao, and L. Zhou, *Laser Photonics Rev.* **15**, 2000492 (2021).
- [48] M. Kim, D. Lee, Y. Yang, Y. Kim, and J. Rho, *Nat. Commun.* **13**, 2036 (2022).
- [49] K. Y. Bliokh, C. Samlan, C. Prajapati, G. Puentes, N. K. Viswanathan, and F. Nori, *Optica* **3**, 1039 (2016).
- [50] H. Dai, L. Yuan, C. Yin, Z. Cao, and X. Chen, *Phys. Rev. Lett.* **124**, 053902 (2020).
- [51] W. Zhu, H. Zheng, Y. Zhong, J. Yu, and Z. Chen, *Phys. Rev. Lett.* **126**, 083901 (2021).
- [52] X. Jiang, J. Tang, Z. Li, Y. Liao, L. Jiang, X. Dai, and Y. Xiang, *J. Phys. D* **52**, 045401 (2018).
- [53] K. Artmann, *Ann. Phys. (Berlin)* **437**, 87 (1948).
- [54] L.-G. Wang and S.-Y. Zhu, *Opt. Lett.* **31**, 101 (2006).
- [55] K. Y. Bliokh and A. Aiello, *J. Opt.* **15**, 014001 (2013).
- [56] J. Wang, M. Zhao, W. Liu, F. Guan, X. Liu, L. Shi, C. T. Chan, and J. Zi, *Nat. Commun.* **12**, 6046 (2021).
- [57] See Supplemental Material at <http://link.aps.org/supplemental/10.1103/PhysRevLett.129.236101> for the methods, derivation, and further discussions on spin Hall effect of light, which includes Refs. [7,58–61].
- [58] H. Haus, *Waves and Fields in Optoelectronics* (Prentice-Hall, Inc., Englewood Cliffs, NJ, USA, 1984).
- [59] S. Fan, W. Suh, and J. D. Joannopoulos, *JOSA A* **20**, 569 (2003).
- [60] J. D. Joannopoulos, S. G. Johnson, J. N. Winn, and R. D. Meade, *Molding the Flow of Light* (Princeton University Press, Princeton, NJ, 2008).
- [61] C. W. Hsu, B. Zhen, M. Soljačić, and A. D. Stone, [arXiv:1708.02197](https://arxiv.org/abs/1708.02197).
- [62] Y. Zhang, M. Zhao, J. Wang, W. Liu, B. Wang, S. Hu, G. Lu, A. Chen, J. Cui, W. Zhang *et al.*, *Sci. Bull.* **66**, 824 (2021).